# Excitation vs electron emission near the kinetic thresholds for grazing impact of hydrogen atoms on LiF(001)

A. Mertens, S. Lederer, K. Maass, and H. Winter*

*Institut für Physik, Humboldt Universität zu Berlin, Invalidenstrasse 110, D-10115 Berlin, Germany*

J. Stöckl, HP. Winter, and F. Aumayr

*Institut für Allgemeine Physik, Technische Universität Wien, Wiedner Hauptstrasse 8-10, A-1040 Vienna, Austria*

The coincident measurement of projectile time-of-flight spectra and number of emitted electrons for grazing scattering of fast $H^0$ atoms from a LiF(001) surface allows us to investigate electronic excitation and emission processes, including those without emission of electrons. Using this method, we are able to study very small electron emission yields and thus kinetic threshold behavior for projectile induced electronic processes. We observe different onsets for electron emission and electronic excitation of the target, providing important conclusions on the relevant interaction mechanisms. Near the kinetic thresholds, inelastic processes are found to be dominated by production of surface excitons.

Recently, considerable attention has been paid to impact phenomena of fast atoms and ions at ionic crystals, i.e., wide-band-gap insulators. Irrespective of the large binding energies of valence band electrons (typically 10 eV), high electron yields,[1–3] low projectile threshold energies for kinetic electron emission,[3,4] substantial negative ion yields,[5–7] and a "metal-like" behavior of electronic stopping of ions down to rather low projectile velocities/energies have been observed.[8,9] A consistent interpretation of these different experimental observations was given in terms of interatomic electron promotion in binary collisions of projectiles with $F^-$ ions at lattice sites of the ionic crystal.[4–6,10–12]

Electron emission and excitation phenomena can be investigated under well defined conditions for impact under a grazing angle of incidence. Then projectiles collide with the surface in a sequence of small angle scattering ("surface channeling"[13]) with specific impact parameters and do not penetrate into the bulk of the target. In this geometry of scattering, we observed for keV protons scattered from a LiF(001) surface discrete energy losses, ascribed to single excitations of valence band electrons, and concluded the formation of negative ions as important precursor in the excitation process.[9] Roncin *et al.*[14] expanded this type of studies by coincident detection of projectile energy loss with the number of emitted electrons. These authors identified from inelastic events accompanied with no electron emission the formation of surface excitons as dominant excitation channel for valence band electrons.

An alternative mechanism for electron emission during grazing impact of hydrogen ions on LiF was proposed by Stracke *et al.*[4] and Zeijlmans van Emmichoven *et al.*[10] from electron spectra for projectile energies of some 100 eV. Here, electron promotion in close $H^0 + F^-$ binary collisions followed by autoionization of doubly excited $F^-$ states are considered to explain emission of electrons at low collision energies (details see below).

We expect important new information on this problem close to the kinetic thresholds for electron excitation and emission. Thus the work reported here, performed with an experimental approach that allows us to measure, in particular, low electron emission yields and electronic excitation probabilities with high sensitivity and accuracy, was intended to help clarify the controversial discussion on the microscopic interaction mechanisms.

We have studied electronic excitation and emission during impact of fast $H^0$ atoms with a flat and clean LiF(001) surface under a grazing angle of incidence $0.5° \leq \Phi_{in} \leq 2°$. Key feature of our setup is the coincident measurement of time-of-flight (TOF) spectra for projectiles scattered from the surface with the number of electrons for each scattering event by means of an electron number (EN) detector. A chopped $H^0$ beam hits the LiF(001) sample under high index ("random") azimuthal orientation. Scattered $H^0$ projectiles are recorded 1.38 m behind the target by means of a channelplate electron multiplier (CEM). Electrons emitted from the LiF surface are collected by a weak electric field owing to a bias of some 10 V applied to a highly transparent grid about 1 cm in front of the target. This grid shields the adjacent high electric field from the bias of a surface barrier detector (SBD) at +30 kV which accelerates the extracted electrons, resulting in detector pulse heights proportional to the electron number ejected per projectile impact.[15] The target surface, kept at a base pressure in the mid $10^{-11}$ mbar range, is prepared by cycles of grazing sputtering with 25 keV $Ar^+$ ions and annealing at about 400 °C.[16] The measurements are performed at about 200 °C, where LiF shows sufficient conductivity, in order to avoid macroscopic charging up of the target.

In our TOF setup, the output signal from a time-to-amplitude converter (TAC) is fed to an analog-to-digital converter (ADC) and stored in the block of a memory unit, with the block address derived via the pulse height of the SBD from a second ADC. Data transfer to the memory unit is triggered at the instant when a projectile recorded by the CEM hits the surface. Because recording of data is initiated by the CEM signal and the efficiency for detection of electrons by the SBD is close to 100%, no corrections

**65** 132410-1
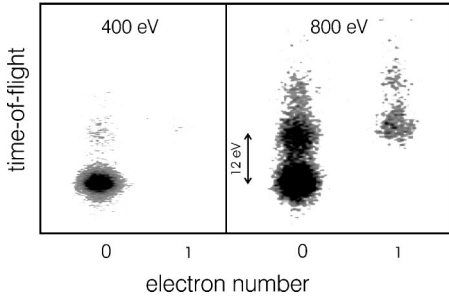
FIG. 1. Projectile time-of-flight versus number of emitted electrons for 400 eV and 800 eV $H^0$ impact at $\Phi_{in}=1.8°$.

for electron number spectra as in studies with the setup as reported in Ref. 14 are necessary. 2D plots in Fig. 1 for 400 eV and 800 eV $H^0$ scattered at $\Phi_{in}=1.8°$ show a number of discrete features for specific electron numbers (horizontal axis) as well as projectile flight time (vertical axis).

The left columns in the plots represent processes with no emission of electrons, where the prominent peak in both cases is due to ''elastic'' events with no electronic excitation of the target and only small energy transfer to lattice atoms of less than 1 eV.[17] The next peak in this column is identified with a longer flight time corresponding to an energy loss of 12.0 eV, and is attributed to the excitation of a surface exciton,[14] i.e., the local excitation of a $F^-$ ion imbedded in the ionic lattice with a binding energy of about 1 eV with respect to vacuum. In the data for 800 eV a weaker signal is found also for the excitation of a second exciton, whereas for 400 eV the inelastic contribution remains rather small. The right columns are related to emission of one electron, where the lowest peak shows a mean energy loss of 14.0 eV. This energy is dissipated by the projectile in lifting an electron from the LiF valence band into vacuum and is larger than for producing an exciton. A weak signal corresponding to the emission of one electron and the additional excitation of one exciton is present in the 800 eV data. For 400 eV, only very few events can be related to the emission of an electron.

Signal patterns as presented in Fig. 1 allow us to investigate the inelastic interaction mechanisms in detail. Owing to the high efficiency for detection of electrons, corrections in the evaluation of data play a negligible role, and precise total electron yields from measured probabilities $W_n$ for the emission of n electrons can be obtained from[15]

$$\gamma=\sum_{n=0}^{\infty} n W_n \bigg/ \sum_{n=0}^{\infty} W_n. \qquad (1)$$

The coincident detection of TOF and EN spectra delivers as well the probability $W_0$ for emission of no electron and makes our method a unique tool for precise measurements near the kinetic emission threshold, where $\gamma$ is very small and $W_0$ dominates. The substantial progress for studies on electron emission achieved with our setup follows from the fact that an EN detector of ''conventional'' design does only provide data for nonzero numbers of electrons, and for small $\gamma$ $W_0$ has to be estimated from assumptions on the statistics of the emission processes.[18]
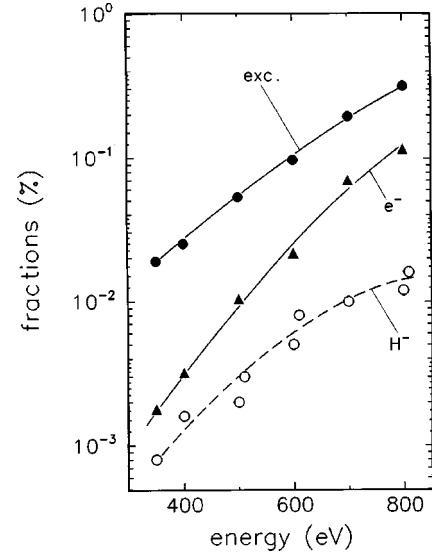


FIG. 2. Fractions of excitons (full circles), emitted electrons (full triangles), and $H^-$ ions (open circles) for scattering of $H^0$ atoms from LiF(001) under $\Phi_{in}=1.8°$ as function of projectile energy.

At $\Phi_{in}=1.8°$ we derive from spectra as shown in Fig. 1 fractions for the excitation of one exciton as well as for emission of one electron (Fig. 2). We determine in addition by means of electric field plates and a further CEM the fractions of negative ions in the scattered beam (positive ion fractions are negligible here) and plot those also in Fig. 2. The data reveal a different kinetic onset behavior for the three quantities, with a dominance of the production of surface excitons. This finding is new and can be used to clarify the relevant interaction mechanisms. In passing we note that the proportionality between electron yield and mean energy loss observed for this system at higher energies ($E>1$ keV) (Refs. 14,19) does not hold near the kinetic threshold.

Electron emission from wide-band gap insulators as LiF is interpreted to proceed in binary collisions of $H^0$ atoms with $F^-$ ions embedded at crystal lattice sites (''active sites''). The two current models for the microscopic interactions are presented in terms of potential curves as sketched in Fig. 3. The upper panel (a) shows calculated potentials as derived in Ref. 10 with a crossing of the diabatic curves for the initial ($H^0+F^-$) and final ($H^-+F^0$) interactions at a distance from the active site of $R\approx4$ a.u. In this model, electron emission proceeds via electron promotion to vacuum (reference for energy scale $H^0+F^0$) at $R<3$ a.u., and population of doubly excited $F^-$ ($F^{-**}$) with subsequent autoionization.[10] In the alternative approach (b), diabatic potential curves for the initial and final interactions do not cross, and $H^-$ is the precursor for excitation of surface excitons ($F^-*$) and electron emission via detachment ($H^0+e^-$) triggered by interactions with lattice atoms surrounding active sites.[5,14] In this qualitative picture, a diabatic curve crossing with the exciton branch ($H^0+F^-*$) is present.[14]

Main features of model (b) were developed to describe the efficient formation of negative ions during grazing scattering of reactive ions from the surface of ionic crystals by
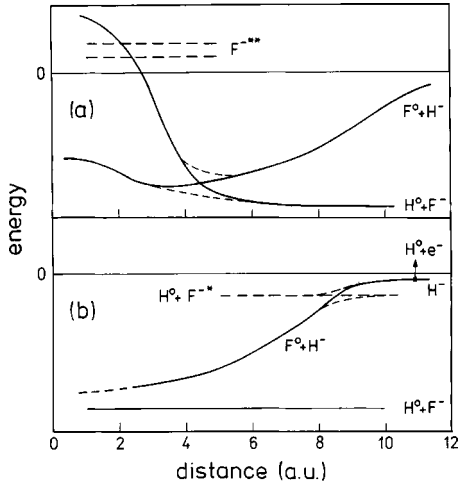
FIG. 3. Sketch of energy diagrams illustrating two models for the interaction of an $H^0$ atom with a LiF(001) surface (details see text).

capture of valence electrons from "active sites" with binding energies $\geq 12$ eV.[5-7,16,20] Capture is mediated by a confluence of levels for the initial (here $F^-$) and final (here $H^-$) states owing to the Madelung potential acting on the active electron.[6] From comparison with recent coupled cluster calculations for $F^-$ formation at LiF,[20] we conclude also for the present situation no crossing of the diabatic potential curves for distances of relevance here, contrary to model (a). In the following we compare the two models with our data.

(1) Projectile trajectories derived from collective interatomic potentials for the Li and F sublattices of the surface using "universal screening"[21] have distances of closest approach $z_{min} \geq 3$ a.u. for our scattering conditions. Then a distance $R \approx 2.5$ a.u. needed in model (a) to promote electrons into vacuum and to crossings with $F^{-**}$ is not reached, and no electron emission can take place.

(2) The probability for electronic transitions in the present collision system can be estimated for the onset region from the data shown in Fig. 2 and amounts to typically 1% or less. For the diabatic curve crossing in model (a) we estimate transition probabilities from Landau-Zener theory[22] (atomic units)

$$P \approx \exp\left( -\frac{\pi}{2v} \Delta E(R_x)^2 \Big/ \frac{d}{dR}(V_{H^-+F^0} - V_{H^0+F^-})_{R_x} \right) \tag{2}$$

with $\Delta E(R_x)$ being the energy gap between the adiabatic potential curves [dashed curves in Fig. 3(a)] at the distance $R_x$ for diabatic curve crossing and $v$ the projectile velocity. From the potential curves given in Ref. 10 we deduce $\Delta E(R_x) = 2.7$ eV $= 0.10$ a.u. as well as the slopes and obtain from Eq. (2) for 400 eV H atoms ($v = 0.127$ a.u.) $P \approx 0.4$ for avoiding the crossing in a single collision. Even without knowledge on the specific collision sequence during surface channeling, such a transition probability would exceed the experimental findings by more than one order of magnitude.
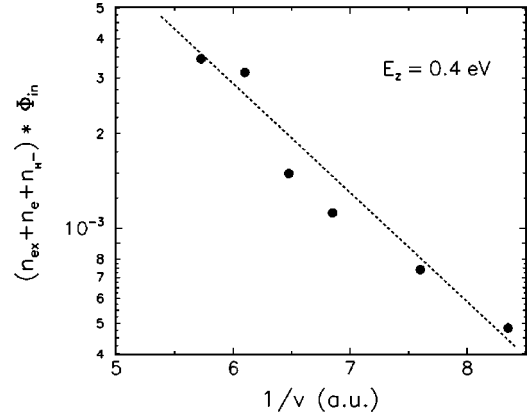


FIG. 4. Plot of $(n_{ex} + n_e + n_{H^-})\Phi_{in}$ versus $1/v$ for constant energy of normal projectile motion $E_z = 0.4$ eV.

In model (b), the transition probability $P_{bin}$ from the initial potential curve (about "parallel" diabatic potential curves in the transition region) can be estimated from the Demkov model[23] which reads for low velocities

$$P_{bin} \approx 2e^{-\pi\alpha\Delta E/v} \tag{3}$$

with $1/\alpha = (\sqrt{E_1} + \sqrt{E_2})/\sqrt{2}$, $E_1$ and $E_2$ being the binding energies of the collision partners and $\Delta E$ the energy defect in the collision. For the specific case mentioned, we find with $\Delta E \approx 4$ eV $= 0.15$ a.u. (see below) from Eq. (3) $P_{bin} \approx 4 \times 10^{-3}$ and, at grazing incidence, the total probability for an effective number of $N$ collisions is $P \approx N P_{bin} \approx 2 - 3\%$ with $N \approx 5 - 8$, in fair agreement with our data.

In model (b), the transition probability to the potential curve $F^0 + H^-$ is directly related to the sum of all fractions in the excitation process ($F^{-*}$, $e^-$, and $H^-$), i.e., $P \approx N$, $P_{bin} = n_{ex} + n_e + n_{H^-}$. Since $\Delta E$ and thus also $P$ depend on the distance from the surface, the distance of closest approach $z_{min}$ has been kept constant for a variation of $v$ by the same energy of projectile motion normal to the surface $E_z = E_0 \sin^2\Phi = 0.4$ eV via tuning of $\Phi_{in}$. Then lengths of trajectories scale according to $1/\Phi_{in}$. Based on Eq. (3) a semilogarithmic plot of $(n_{ex} + n_e + n_{H^-})\Phi_{in}$ versus $1/v$ for $350$ eV $\leq E \leq 800$ eV ($1.91^0 \geq \Phi_{in} \geq 1.31°$) shows in Fig. 4 the expected linear behavior. From the slope
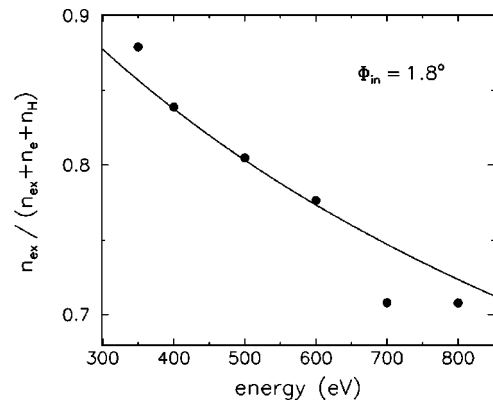


FIG. 5. Plot of $(n_{ex})/(n_e + n_{ex} + n_{H^-})$ versus projectile energy for $\Phi_{in} = 1.8°$. Solid curve: description of data using Eq. (2).

$-\pi\alpha\Delta E$ we deduce $\Delta E = (4.0 \pm 0.5)$ eV which is consistent with an estimate based on a lowering of the $H^-$ binding energy by the Coulomb potential owing to the hole at the active site and by the dielectric response.[5–7] The effective number of collisions is deduced to $5.3 \leq N \leq 7.8$.

In the second step, the specific fractions in the excitation result from the curve crossing on the outgoing path at distances $\geq z_{min}$. Then the different kinetic threshold behavior for exciton production and electron emission is interpreted by an avoided crossing of the adiabatic potential curves [See Fig. 3(b)]. We expect that the potential parameters in Eq. (2) show only a weak dependence on the collision geometry so that, e.g., the relative exciton yield $(n_{ex})/(n_{ex} + n_e + n_{H^-})$ is given by $1 - P = 1 - \exp(-c/v)$. Experimental exciton yields as function of projectile energy as shown in Fig. 5 are well fitted by $1 - P$ with $c \approx 0.22$ a.u. With a rough

estimate of about 1 eV/a.u. for the difference in slope of the potential curves, we derive from Eq. (2) for the separation of the adiabatic potential curves $\Delta E(R_x) \approx 2$ eV.

In conclusion, for hydrogen atoms grazingly scattered from LiF(001) absolute fractions have been determined for the production of excitons, electrons, and $H^-$ ions at their respective onset energies. Our sensitive measurements show that $H^-$ formation is the precursor for exciton as well as electron production and thus rule out an earlier proposed alternative model. The relevant inelastic transition processes have been analyzed in a quantitative manner.

*Author to whom correspondence should be addressed. Electronic address: winter@physik.hu-berlin.de

[1] J. Schou, Scanning Microsc. **2**, 607 (1988).

[2] D. Hasselkamp, in *Particle Induced Electron Emission II*, Springer Tracts on Modern Physics No. 123 (Springer, Berlin, 1992), p. 1.

[3] M. Vana *et al.*, Europhys. Lett. **29**, 55 (1995).

[4] P. Stracke *et al.*, Nucl. Instrum. Methods Phys. Res. B **125**, 657 (1997).

[5] C. Auth *et al.*, Phys. Rev. Lett. **75**, 2292 (1995).

[6] A. G. Borisov *et al.*, Phys. Rev. Lett. **77**, 1893 (1996).

[7] A. G. Borisov and V. Sidis, Phys. Rev. B **56**, 10 628 (1997).

[8] K. Eder *et al.*, Phys. Rev. Lett. **79**, 4112 (1997).

[9] C. Auth *et al.*, Phys. Rev. Lett. **81**, 4831 (1998).

[10] P.A. Zeijlmans van Emmichoven *et al.*, Phys. Rev. B **59**, 10 950 (1999).

[11] S. Zamini *et al.*, Surf. Sci. **417**, 372 (1998).

[12] R. Souda, Int. J. Mod. Phys. B **14**, 1139 (2000).

[13] D.S. Gemmell, Rev. Mod. Phys. **46**, 129 (1974).

[14] P. Roncin *et al.*, Phys. Rev. Lett. **83**, 864 (1999).

[15] F. Aumayr *et al.*, Appl. Surf. Sci. **63**, 177 (1999).

[16] H. Winter, Prog. Surf. Sci. **63**, 177 (2000).

[17] A. Mertens and H. Winter, Appl. Surf. Sci. **47**, 139 (1991).

[18] M. Vana, F. Aumayr, C. Lemell, and HP. Winter, Int. J. Mass Spectrom. Ion Processes **149/150**, 45 (1995).

[19] H. Eder *et al.*, Phys. Rev. A **62**, 052901 (2000).

[20] A.G. Borisov *et al.*, Phys. Rev. B **63**, 045407 (2001).

[21] J.F. Ziegler *et al.*, *The Stopping and Range of Ions in Solids* (Pergamon Press, New York, 1985).

[22] R. E. Johnson, *Atomic and Molecular Collisions* (Plenum Press, New York, 1982), p. 116.

[23] Y. N. Demkov, Sov. Phys. JETP **18**, 138 (1964).